

# Ber And SNR Comparisons For 8, 16 And 64 Qam Modulation Schemes Through Rain Affected Air Interface Channel

Akingbade Kayode<sup>#1</sup>, F and Alo Opeyemi, O<sup>\*2</sup>

Electrical and electronics engineering, Federal University of Technology, Akure  
P.M.B 704, Ilesha-Akure Expressway, Akure-Ondo state Nigeria

## Abstract

One major drawback of the use of satellite communications is that, at frequencies above 10 GHz (that is, the K-bands and above), some atmospheric disturbances such as rain, snow, and beam spread, greatly affect the quality of the transmitted signals. A number of approaches have been proposed to combat this drawback, some of which include the use of site diversity, reconfigurable antenna pattern, frequency diversity, terrestrial backup and power control. However, these approaches have inherent limitations in terms of resources. This paper centers on the performance analysis of 8-QAM, 16-QAM and 64-QAM modulations schemes in terms of attenuation, bit error rates, Signal-Noise ratio (SNR) and, data throughputs under different rain attenuation profiles. The modulation was carried out using Rectangular QAM modulation scheme, where the values of M was varied from 8, 16 and 64 and the demodulation of the transmitted signal was achieved by raising the received signal to fourth power before passing through a band pass filter. The results obtained from the simulation carried out shows that the bit error rates performance of 8-QAM is the best without and with rain attenuation which implies that 8-QAM has a better performance in that its BER is low compared with 16-QAM and 64-QAM. It could also be deduced that, the more the transmitting power (SNR) the lesser the error (BER) at any value of SNR.

**Keywords:** QAM modulation, quadrature, attenuation, Bit error rate (BER), signal to noise ratio (SNR).

## I. INTRODUCTION

Quadrature amplitude modulation (QAM) is the modulation scheme being used by most digital cable channels for transmission. These channels are encoded and then transmitted through television service providers, such as Digital TV, to their destination [4].

QAM modulation is both an analog and a digital modulation scheme that transmits either two

analog message signals or digital signals by varying the amplitude of the carrier signal through amplitude modulation [4]. These two carrier waves are called quadrature carriers because they are out of phase with each other by 90 degrees, the modulated signal is the summation of both phase shift keying and amplitude shift keying [1], [5]. QAM scheme is popular among telecommunication system providers because of their high spectral efficiencies based on the chosen constellation size. M-ARY QAM modulation is a type of modulation that makes use of different M-number of modulation schemes depending on the pre-set conditions [3], [5].

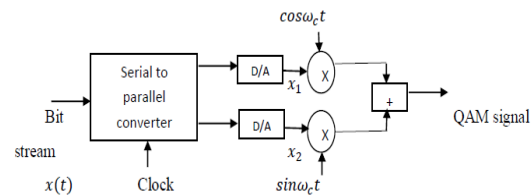


Figure 1: Generation of QAM signal (Source: Arne, 2007)

Assuming the two message signals are  $x_1(t)$  and  $x_2(t)$ .  $x_1(t)$  is multiplied in phase with  $\cos\omega_c t$  and the second message signal  $x_2(t)$  is multiplied in quadrature with  $\sin\omega_c t$ , both signals are then added to obtain the QAM signals just as illustrated in the Figure 1.

Mathematically, QAM expression is as given in equation (1)

$$V_{QAM}(t) = x_1(t)\cos\omega_c t + x_2(t)\sin\omega_c t \quad (1)$$

Coherent detection is done at the receiver side to recover the original signal sent, low pass filtering removes the high frequency components leaving the needed signals. The advantages QAM has over the other forms of data modulation is that it efficiently manages the bandwidth and it is able to carry higher data rates. Analog QAM is used in NTSC and PAL televisions whereby the components of Chroma are

carried simultaneously while digital QAM is used in radio communication systems. QAM disadvantages includes susceptibility to noise, because it needed linear amplifiers to maintain linearity, it consumes more power [6].

## II. MODULATION AND DEMODULATION SIMULATION

The modulation was carried out using Rectangular QAM modulation scheme, where the values of M was varied from 8, 16 and 64. QAM modulation uses two quadrature carriers in transmitting signal therefore, to transmit 16 different possible bits will be achieved by using symbol of 4 bits, that is,  $2^N$  where  $N=4$  [2], [5]. Therefore QAM can be used to generate  $2^N$  possible distinguishable symbols. The illustration is as given in equation (2)

$$V_{QASK}(t) = A_e(t)\sqrt{P_s}\cos\omega_c t + A_0(t)\sqrt{P_s}\sin\omega_c t \quad (2)$$

Where  $A_e(t)$  and  $A_0(t)$  are the two quadrature amplitudes of the QAM modulator,

$\sqrt{P_s}\cos\omega_c t$  and  $\sqrt{P_s}\sin\omega_c t$  are the two carriers, and

$P_s$  is the transmitting power of the signal.

Table 1 depicts the various M-QAM modulation types and their respective schemes.

**Table 1: Types of QAM**

Name of scheme	Bits per symbol	Number of symbols
4-QAM	2	$2^2 = 4$
8-QAM	3	$2^3 = 8$
16-QAM	4	$2^4 = 16$
32-QAM	5	$2^5 = 32$
64-QAM	6	$2^6 = 64$

To demodulate the transmitted signal of QAM modulation, the received signal was first raised to fourth power after which a band pass filter with a center frequency coupled with a frequency divider to recover the quadrature carriers as given in equation (3)

$$V_{QASK}^4(t) = P_s^2 [A_e(t) \cos \omega_c t + A_0(t) \sin \omega_c t]^4 \quad (3)$$

The signal is then passed through a band pass filter

Therefore the resulting equation (4)

$$V_{QASK}^4(t) = \frac{P_s^2}{8} [A_e^4(t) + A_0^4(t) - 6A_e^2(t)A_0^2(t)] \cos 4\omega_c t + Ps2Ae(t)A0(t)Ae2t-A02(t)\sin 4\omega ct \quad (4)$$

The Table 2 shows for different Rain diameter range the implementation of the system by varying the modulation schemes and the resultant attenuation range in (dB)

**Table 2: showing the rain attenuation with different modulation schemes**

Rain Diameter (d/mm)	Attenuation (dB)	Modulation Scheme
$0 \leq d \leq 0.1 \text{ mm}$	$0 < \alpha < 0.10$	64-QAM, 16-QAM, 8-QAM
$0.1 \text{ mm} < d \leq 0.5 \text{ mm}$	$0.1 < \alpha < 4.50$	64-QAM, 16-QAM, 8-QAM
$0.5 \text{ mm} < d \leq 1.0 \text{ mm}$	$0.1 < \alpha < 4.50$	64-QAM, 16-QAM, 8-QAM
$1.0 \text{ mm} < d \leq 1.5 \text{ mm}$	$0.1 < \alpha < 4.50$	64-QAM, 16-QAM, 8-QAM
$1.5 \text{ mm} < d \leq 2.0 \text{ mm}$	$0.1 < \alpha < 4.50$	64-QAM, 16-QAM, 8-QAM
$2.0 \text{ mm} < d \leq 2.5 \text{ mm}$	$4.50 < \alpha < 7.00$	16-QAM, 8-QAM
$2.5 \text{ mm} < d \leq 3.0 \text{ mm}$	$4.50 < \alpha < 7.00$	16-QAM, 8-QAM
$3.0 \text{ mm} < d \leq 3.5 \text{ mm}$	$4.50 < \alpha < 7.00$	16-QAM, 8-QAM
$3.5 \text{ mm} < d \leq 4.0 \text{ mm}$	$7.00 < \alpha < 10.00$	8-QAM
$4.0 \text{ mm} < d \leq 4.5 \text{ mm}$	$7.00 < \alpha < 10.00$	8-QAM
$4.5 \text{ mm} < d \leq 5.0 \text{ mm}$	$7.00 < \alpha < 10.00$	8-QAM
$d > 5.0 \text{ mm}$	$\alpha > 10.00$	8-QAM

## III. RAIN DROPS SIZE DISTRIBUTION

The drop size distribution was derived from the raw power received by the radar given in equation (5)

$$p(f_D)\Delta f_D = C(r) \frac{1}{r^2} \frac{1}{\Delta h} \eta(f_D)\Delta f_D \quad (5)$$

where  $\Delta h$  is the range (height) resolution,  $r$  is the number of the range gate,  $C(r)$  is a calibration function containing radar specific parameters,  $\eta(f_D)\Delta f_D$  is the spectral reflectivity density, that is, the backscatter cross section per volume and per frequency, and  $\Delta f_D$  is the frequency resolution.

The Doppler Spectra are resolved into 64 lines as given in equation (6)

$$\eta_{nn} = 10^{F_{nn}/10} \quad (6)$$

where  $nn$  indicates the line number ( $0 \leq nn \leq 63$ ),  $F_{nn}$  is called logarithmic spectral volume reflectivity. The spectral reflectivity density is then defined in equation (7)

$$\eta(f_{D,nn}) = \frac{\eta_{nn}}{\Delta f_D} \quad (7)$$

where  $\Delta f_D = 30.52 \text{ Hz}$

Using the generalized form, in which the height dependent density correction for the fall velocity  $dv(h)$  Atlas (1973) is defined in equation (8)

$$v(D) \text{ m/s} = (9.65 - 10.3 \exp(-0.6D)) \partial v(h) \text{ for } 0.109 \leq D \leq 6 \text{ mm} \quad (8)$$

Using the America Standard Atmosphere conditions for the height dependence of air density and making use of the relation of [8]  $\partial v(h)$  under these assumptions is defined as in equation (9)

$$\partial v(h) = [1 + 3.68 \times 10^{-5} h + 1.71 \times 10^{-9} h^2] \quad (9)$$

where  $h$  is given as height

The spectra reflectivity can also be calculated from the drop diameter using the expression given in equation (10)

$$\eta(D_{nn}) = \eta(f_{D,nn}) \frac{\partial f_D}{\partial v} \frac{\partial v}{\partial D} \quad (10)$$

where

$$\frac{\partial f_D}{\partial v} = 160.1973 \text{ m}^{-1} \quad (11)$$

and

$$\frac{\partial v}{\partial D} (\text{ms}^{-1} \text{ mm}^{-1}) = 6.18 \times \exp(-0.6D) \partial v(h) \quad (12)$$

Substituting equation (10) and (11) into (12) gives the expression in equation (13)

$$\eta(D_{nn}) \text{ m}^{-1} \text{ mm}^{-1} = \eta(f_{D,nn}) \times 990.02 \times \exp(0.6 \text{ mm}^{-1} D) \quad (13)$$

Dividing equation (13) by  $\sigma(D_{nn})$  gives the expression in equation (14)

$$N(D_{nn}) = \frac{\eta(D_{nn})}{\sigma(D_{nn})} \quad (14)$$

where  $N(D_{nn})$  is the Drop size distribution, and

$\sigma(D_{nn})$  is the single particle backscattering cross section of rain drop of diameter  $D_{nn}$ .

#### IV. EQUIVALENT RADAR REFLECTIVITY FACTOR

The equivalent radar reflectivity factor is defined by the equation given in (15)

$$Z_e = \frac{\lambda^4}{\pi^5 |K|^2} \int_0^\infty \eta(f_{D,m}) \partial f_D \quad (15)$$

where  $\lambda$  is the radar wavelength,

$|K|^2$  is the dielectric factor of water which is 0.93,

$\eta(f_D)\Delta f_D$  is the spectral reflectivity density, and

$\eta$  is radar reflectivity per unit volume.

In the limit of small drops (Rayleigh approximation),  $Z$  is equal to the 6<sup>th</sup> moment of the drop size distribution in equation (16)

$$Z = \int_0^\infty N(D) D^6 dD \quad (17)$$

where  $N(D)dD$  is the number of drops per unit volume with diameters in the interval  $dD$ ,

$Z$  is calculated on the basis of the drop size distribution measured by the Micro Rain Radar using equation (17).

#### V. RAIN RATE

This is the rate at which water reaches the ground or the rate of accumulation of water per unit time ( $\text{mm/hr}$ ). It is also defined as the number of raindrops falling in a particular region per unit time. It is measured in  $\text{mm/hr}$ . The differential rain rate is equal to the volume of the differential droplet number density multiplied with the terminal falling velocity  $v(D)$ . Where the differential droplet number density is given in equation (18)

$$D_N = \left( \frac{\pi}{6} N(D) D^3 \right) \quad (18)$$

From this product, the rain rate is obtained by integrating over the drop size using the formula given in equation (19)

$$RR = \frac{\pi}{6} \int_0^\infty N(D) D^3 V(D) dD \quad (19)$$

#### VI. LIQUID WATER CONTENT (LWC)

The liquid water content is the product of the total volume of all droplets with the density of water  $\rho_w$ , divided by the scattering volume. It is therefore proportional to the third moment of the drop size distribution. This is calculated by using the formula given in equation (20):

$$Lwc = \rho_w \frac{\pi}{6} \int_0^\infty N(D) D^3 dD \quad (20)$$

Having obtained the parameters above through the equations, it is then imperative to discuss how the

rain cell size is related to the signal wave length passing through it. It has been revealed that, signal attenuation during rain events occurs when the wavelength of the signal being propagated is less than the diameter of the rain drop. It then gets absorbed by the rain cell when it passes through it [7]. This phenomenon, also known as scattering, results when the rain cell diameters are larger than the wavelengths of the transmitted signals.

### VII. SCATTERING OF SIGNALS BY RAIN DROPS

Scattering of signals by rain drops is also known as depolarization of signals which is caused by the differential attenuation and differential phase shift by different rain drop sizes [10]. These above scattering parameters can be deduced by estimating the forward scattering of rain drop [11] as given in equations (21) and (22)

Differential attenuation is given by

$$\Delta A = 8.686 \times \text{Im}(K_h - K_v)L \quad (21)$$

While differential phase shift is given by

$$\Delta \phi = \left[ \frac{180}{\pi} \right] \times \text{Re}(K_h - K_v)L \quad (22)$$

where  $K_h$  is the horizontal component of propagation constant,  $K_v$  is the vertical component of propagation constant, and

$L$  is the path length through the medium. This path length is taken to be 5.4 km according to [11] in their research and the expression given to these parameters is as indicated in equation (23)

$$K_{h,v} = \left( \frac{2\pi}{\lambda} \right) \int f_{h,v} n(a) da \quad (23)$$

Where  $f_{h,v}$  denotes the forward scattering amplitudes in both horizontal and vertical direction for rain drops with DSD  $n(a)$  and  $a$  is the equivolumetric radius of a drop of rain.

Often times this fading effect is caused by the shape of the rain drop which is also related to fall velocity and drop breakup and also by the rain intensity. This theory was postulated from the measurements that were made while the rain drops were falling in the air stream of a vertical wind tunnel, and some were made when the drops attained their terminal velocity after falling from a sufficient height (~12m) in stagnant air [7]. From the experiment carried out by [9], it was revealed that water drops above 1.0mm in radius were of oblate spheroids shape with a flattened base and those below were spherical in shapes which least affects signal propagation. [9] were able to establish the fact that as a result of the presence of water vapor molecules, water droplets cause signal attenuation. Attenuation is determined not by how much rain that is falling, but by the size of the rain cell diameter.

This rain attenuation is obtained step wisely as shown below:

The height of the  $h_R$  in (Km) is as given in equation (24)

$$h_R = h_o + 0.36 Km \quad (24)$$

where  $h_o$  is the 0°C Isotherm height above sea level [15].

The slant path  $L_S$ , below the freezing rain height is as indicated in equation (25)

$$L_S = \frac{(h_R - h_s)}{\sin \theta} (Km) \quad (25)$$

where  $h_s$  is the location height (Km) above sea level,

$\theta$  is angle of elevation of the micro rain radar or disdrometer measured in degrees.

To realize a better accuracy of slant path using elevation angles less than 5°, then the equation (26) is preferred

$$L_S = \frac{2(h_R - h_s)}{\left[ \sin^2 \theta + \frac{2(h_R - h_s)}{Re} \right]^{0.5} + \sin \theta} (Km) \quad (26)$$

where  $Re = 8500Km$ . [12].

The horizontal projection  $L_G$ , of the slant path length is given by equation (27) as

$$L_G = L_S \cos \theta \text{ in } Km \quad (27)$$

The rain intensity,  $R_{0.01} (mm/hr)$ , exceeded for 0.01% of an average year, using 1- min integration time from the rain rate data is used to calculate the specific attenuation  $\gamma_R$  in equation (28)

$$\gamma_R = K (R_{0.01})^\alpha \text{ in } dB/Km \quad (28)$$

where  $K$  and  $\alpha$  parameters are dependent on rain drop size distribution, frequency and polarization of the signal, and rain temperature which could be obtained from [15].

where  $K$  is given by equation (29)

$$K = \frac{[K_H + K_V + (K_H - K_V) \cos^2 \theta \cos(2t)]}{2} \quad (29)$$

And  $\alpha$  is determined from equation (30)

$$\alpha = \frac{[K_H \alpha_H + K_V \alpha_V + (K_H \alpha_H - K_V \alpha_V) \cos^2 \theta \cos(2t)]}{2K} \quad (30)$$

where  $K_H$  is propagation constant in the horizontal plane,

$K_V$  is the propagation constant in the vertical plane, and  $t$  parameter is the angle of polarization tilt with respect to the horizontal ( $t = 45^\circ$  for circular polarization).

Also the horizontal path adjustment factor,  $r_{0.01}$  for 0.01% Of the time is calculated using equation (31)

$$r_{0.01} = \frac{1}{1+0.78 \sqrt{\frac{L_G \gamma_R}{f} 0.38 [1-e^{-2L_G}]}} \quad (31)$$

where  $f$  is frequency in (GHz)

The adjusted rainy path length,  $L_R$  (Km), through rain is now given as shown in equation (32)

$$L_R = \frac{L_G r_{0.01}}{\cos \theta} \text{ for } \varepsilon > \theta \quad L_S = \frac{(h_R - h_S)}{\sin \theta} \text{ for } \varepsilon \leq \theta \quad (32)$$

where  $\varepsilon$  is given by equation (33)

$$\varepsilon = \tan^{-1} \left[ \frac{h_R - h_S}{L_G r_{0.01}} \right] \quad (33)$$

and the vertical reduction factor,  $V_{0.01}$  for 0.01% of the time is given in equation (34)

$$V_{0.01} = \frac{1}{1 + \sqrt{\sin \theta} \left[ 31 \left( 1 - e^{-\frac{\theta}{1+\chi}} \right) \sqrt{\frac{L_R \gamma_R}{f^2}} - 0.45 \right]} \quad (34)$$

where:

$$\chi = 36 - /\phi/, \text{ for } /\phi/ < 36^\circ \text{ and } \chi = 0, \text{ for } /\phi/ \geq 36^\circ \quad (35)$$

where  $\chi$  and  $\phi$  are constants

Equation (36) gives the effective path length  $L_E$  (Km) through rain

$$L_E = L_R V_{0.01} \quad (36)$$

The predicted attenuation exceeded for 0.01% for an average year is given in equation (37)

$$A_{0.01} = \gamma_R L_E (dB) \quad (37)$$

The attenuation estimated to be exceeded for the other percentages of an average year, in the range 0.001% to 10% is then obtained from the attenuation to be exceeded for 0.01% for an average year a given in equation (38)

$$A_P = A_{0.01} \left( \frac{P}{0.01} \right)^{-[0.655 + 0.33 \ln(P) - 0.045 \ln(A_{0.01}) - W \sin \theta (1-P)]} \quad (38)$$

where  $P$  is the percentage probability of interest and  $W$  is given in equation (39) and (40)

for  $P \geq 1\%$ ,  $W = 0$

for  $P < 1\%$ ,  $W = 0$  for  $/\phi/ \geq 36^\circ$

$$W = -0.005(/\phi/ - 36) \text{ for } \theta \geq 25^\circ \text{ and } /\phi/ < 36^\circ \quad (39)$$

$$W = -0.005(/\phi/ - 36) + 1.8 - 4.25 \sin \theta, \text{ for } \theta < 25^\circ \text{ and } /\phi/ < 36^\circ \quad (40)$$

Rain attenuation is calculated using the power law relation given in equation (41)

$$A = aR^b \quad (41)$$

Where “ $a$ ” and “ $b$ ” are the regression coefficients given by [13], [14].

where  $a = 12.2903$  and  $b = 0.2973$

for the frequency range of 1-100 GHz.

## VIII. RESULTS

Figure 2 shows attenuations at 1-5 dB using 64-QAM modulation scheme, at SNR of 30 dB, 1 dB attenuation has a BER of  $10^{-6.7}$ , while 2 dB attenuation has a BER of  $10^{-5.7}$ , 3 dB attenuation has a BER of  $10^{-5.6}$ , 4 dB attenuation has a BER of  $10^{-5.5}$ , 5 dB attenuation has a BER of  $10^{-5.45}$ .

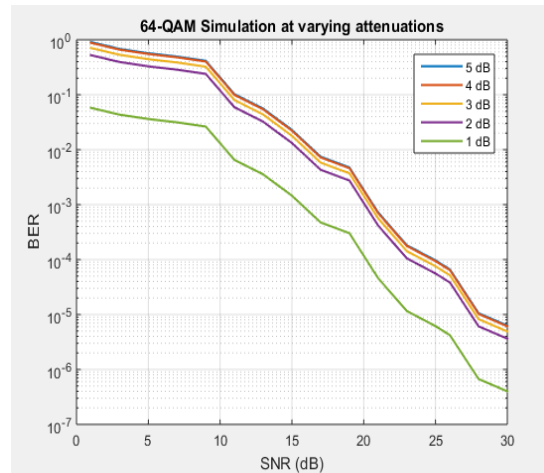
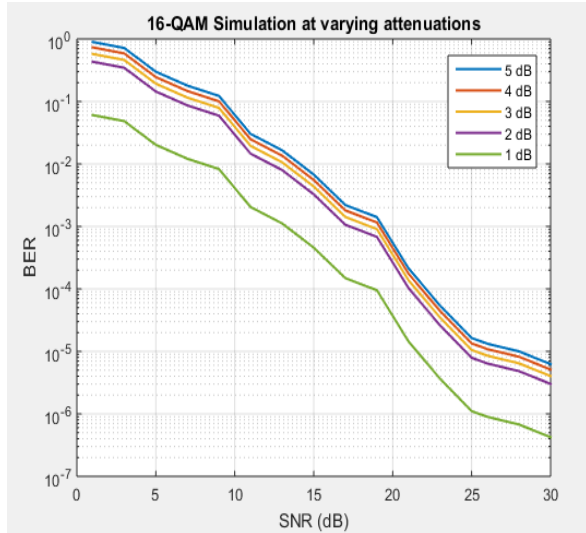


Figure 2: 64-QAM simulation at varying attenuations





**Figure 3: 16-QAM simulation at varying attenuations**

Figure 3 shows attenuations at 1-5 dB using 16-QAM modulation scheme, at SNR of 30 dB, 1 dB attenuation has a BER of  $10^{-6.65}$ , while 2 dB attenuation has a BER of  $10^{-5.8}$ , 3 dB attenuation has a BER of  $10^{-5.7}$ , 4 dB attenuation has a BER of  $10^{-5.6}$ , 5 dB attenuation has a BER of  $10^{-5.5}$ .

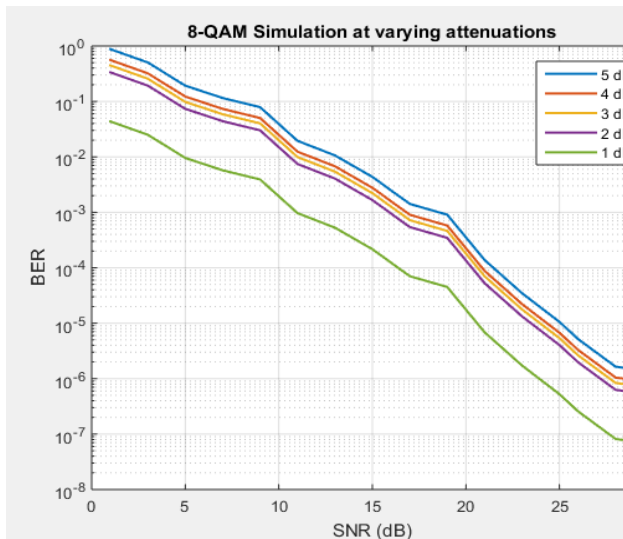


**Figure 4: 8-QAM simulation at varying attenuations**

Figure 4 shows attenuations at 1-5 dB using 8-QAM modulation scheme, at SNR of 30 dB, 1 dB attenuation has a BER of  $10^{-7.4}$  while 2 dB attenuation has a BER of  $10^{-6.6}$ , 3 dB attenuation has a BER of  $10^{-6.4}$ , 4 dB attenuation has a BER of  $10^{-6.1}$ , 5 dB attenuation has a BER of  $10^{-5.9}$ .

From Figures 2-4, it can be deduced that the higher the attenuation the higher the BER. The performances of these modulation schemes was also compared and the results is as shown in the Figures 5-9.

Figure 5 shows attenuation at 1 dB, at 30 dB SNR, 8-QAM has a BER of  $10^{-7.4}$ , 16-QAM has a BER of  $10^{-6.7}$ , and 64-QAM has a BER of  $10^{-6.7}$ .

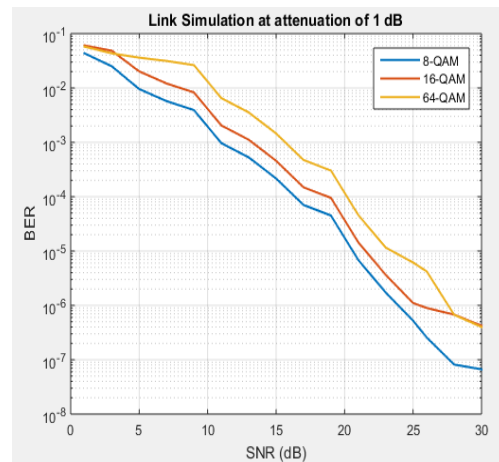


**Figure 5: Link simulation at attenuation of 1 dB**

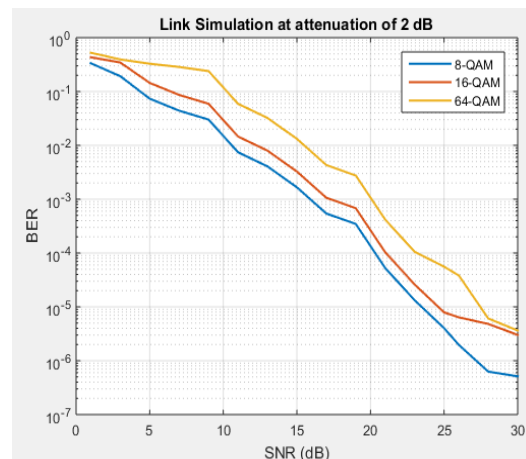


**Figure 6: Link simulation at attenuation of 2 dB**

Figure 6 shows attenuation at 2 dB, at 30 dB SNR, 8-QAM has a BER of  $10^{-6.6}$ , 16-QAM has a BER of  $10^{-5.8}$ , and 64-QAM has a BER of  $10^{-5.7}$ .

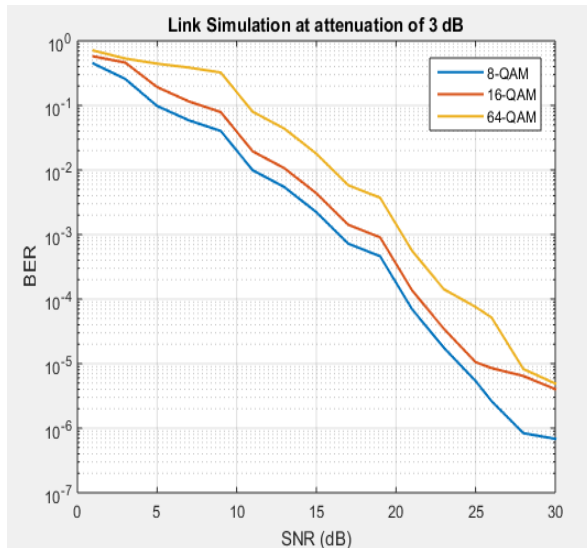


Figure 7: Link simulation at attenuation of 3 dB

Figure 7 shows attenuation at 3 dB, at 30 dB SNR, 8-QAM has a BER of  $10^{-6.4}$ , 16-QAM has a BER of  $10^{-5.7}$ , and 64-QAM has a BER of  $10^{-5.6}$ .

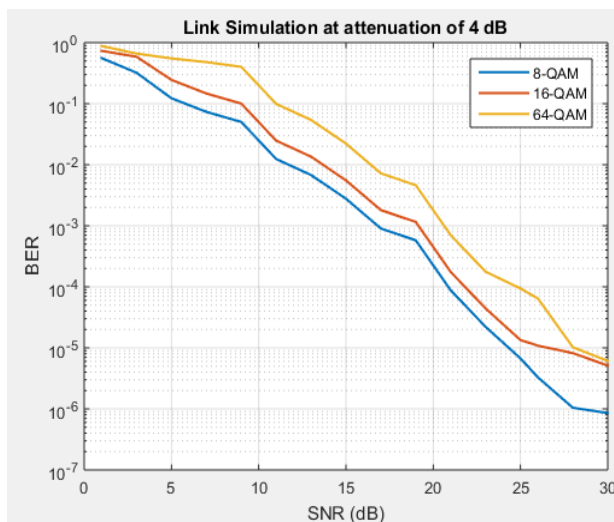


Figure 8: Link simulation at attenuation of 4 dB

Figure 8 shows attenuation at 4 dB, at 30 dB SNR, 8-QAM has a BER of  $10^{-6.1}$ , 16-QAM has a BER of  $10^{-5.6}$ , and 64-QAM has a BER of  $10^{-5.5}$ .

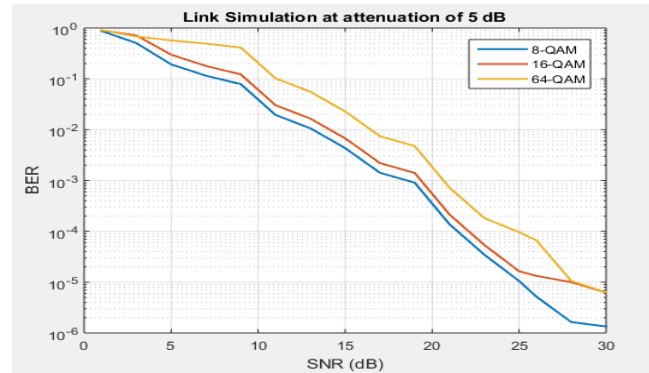


Figure 9: Link simulation at attenuation of 5 dB

Figure 9 shows attenuation at 5 dB, at 30 dB SNR, 8-QAM has a BER of  $10^{-5.8}$ , 16-QAM has a BER of  $10^{-5.5}$ , and 64-QAM has a BER of  $10^{-5.4}$ . It can be deduced from Figures 5-9 that 8-QAM has better performance in terms of BER compared to 16-QAM and 64-QAM modulations at any level of attenuation.

## IX. CONCLUSION

The simulation results showed that the higher the attenuation the higher the BER and the BER increases with increase in the order of the M-ARY QAM modulation. That is, with reduction in the Euclidean distance between the constellation points. Hence, the bit error rates performance of 8-QAM is the best without and with rain attenuation which implies that 8-QAM has a better performance in that its BER is low compared with 16-QAM and 64-QAM. It could also be deduced that, the more the transmitting power (SNR) the lesser the error (BER) at any value of SNR.

## REFERENCES

- [1] John G. Proakis and Masoud Salehi (2013). Digital Communications Fifth edition.. Irwin Electronics & Computer Engineering
- [2] Ahmed, Z., Mohammed, R., Mahdi, A., and Mukhammed, M. (2014). Communication Satellites. UNMC Group project, BPA Module.
- [3] Ajewole, M.O., Kolawole, L.B., Ajayi, G.O. (1999). Theoretical Study of the Effect of Different Types of Tropical Rainfall on Microwave and Millimeter-wave Propagation. Radio Science, 34(5), 1103-1124.
- [4] Arne, S. (2007). An Introduction to Adaptive QAM Modulation Schemes for Known and Predicted Channels. Proceedings of the IEEE | Vol. 95, No. 12.
- [5] Andrea, J., and Soon-Ghee, C. (1998). Adaptive Coded Modulation for Fading Channels. IEEE transactions on communications, vol. 46, No. 5, 595
- [6] Maurologoitia, A., Riera, J. M., Garcia, P. and Benarroch, A.(2006). Performance of Fade Mitigation Techniques in a Fixed 48GHz. International Journal of Wireless Information Networks, Vol 13, Issue 1, pp 19 – 30.
- [7] Okamura, S., and Oguchi, T. (2010). Electromagnetic wave Propagation in Rain and Polarization Effects. Proceedings of Japan Academy Series 3 Physical and Biological Sciences.

- [8] Foote, G.B., and duToit, D.S. (1969). Terminal Velocity of Raindrops aloft. *Journal of Meteorology*, 8, 249-253.
- [9] Muhammed Z., Zaffer, H., Shahid, A.K., Jamal, N. (2011). Atmospheric Influences on Satellite Communications. *Electrical Review*.
- [10] Aderemi, S. A. (2008). Computation of the Scattering Parameters Using Indian Lognormal Dropsizes Distribution at 16,19.3 and 34.8 GHz for Spherical and Oblate Spheroidal Rain Models. *Asian Journal of Scientific Research*, 1(3), 213-221.
- [11] Animesh, M. and Arpita, A. (2011). Ku-Band Signal Depolarization over Earth-Space Path in Relation to Scattering of Raindrops at at Tropical Location. *IEEE*.
- [12] Ojo, J.S., Ajewole, M.O., Sakar, S.K. (2008). Rain Rate and Rain Attenuation Prediction for Satellite Communication in Ku and Ka bands over Nigeria. *Progress in Electromagnetics Research B*,(5), 207-223.
- [13] Chebil, J., and Rahman, T.A. (1999). Development of 1 min Rain rate Contour Maps for Microwave Applications in Malaysia Peninsula. *Electronics Letters*, 35, 1712-1774.
- [14] Ajewole, M.O., Kolawole, L.B., Ajayi, G.O. (1999). Theoretical Study of the Effect of Different Types of Tropical Rainfall on Microwave and Millimeter-wave Propagation. *Radio Science*, 34(5), 1103-1124.
- [15] ITU-R P.838-3. (2005). Specific Attenuation Model of Rain for Use in Prediction Methods.